Atomic force microscopy of cellulose microfibrils: comparison with transmission electron microscopy

Shaune J. Hanley, Julie Giasson, Jean-François Revol and Derek G. Gray*
Pulp and Paper Research Institute of Canada and Department of Chemistry, McGill University, 3420 University St, Montreal, Quebec, Canada H3A 2A7

Atomic force microscopy (AFM) and transmission electron microscopy (TEM) have been used to image well-characterized algal cellulose microfibrils. Cross-sections of the microfibrils observed by TEM are square, whereas the AFM topography of these microfibril surfaces shows a rounded profile due to convolution with the shape of the AFM tip. Height and base width measurements taken from cross-sections of these AFM micrographs also show a marked dependence on the scan rate of the AFM tip. AFM images of the surface of the highly crystalline cellulose microfibrils were obtained at atomic resolution under ambient conditions; the images showed periodicities along the microfibril axis of 1.07 and 0.53 nm that may correspond to the fibre and glucose unit repeat distances, respectively.

(Keywords: atomic force microscopy; cellulose microfibrils; transmission electron microscopy)

Introduction

The atomic force microscope[1] can profile surfaces at resolutions down to the atomic level[2]. It operates[3] by scanning the sample under a sharp tip mounted on a flexible cantilever with a spring constant of the order of $0.5 \, N \, m^{-1}$. An optical detection system is used to detect the deflection of the cantilever, allowing force or height measurements of the surface. A topographic image can be generated from repeated line scans across the surface. In this communication, we examine atomic force microscopy (AFM) images of well-characterized natural cellulose microfibrils, in order to gain insight into the potential and limitations of the AFM method.

Cellulose, the main constituent of plant cell walls, exists as microfibrils of indefinite length. In green algae such as *Valonia ventricosa*, the cellulose microfibrils are highly crystalline and of large cross-section[4]. Well-resolved high resolution diffraction contrast images have been obtained by transmission electron microscopy (TEM) on ultra-thin transverse sections of these native cellulose microfibrils[5]. The images show that the microfibrils are perfect crystals having nearly square cross-section with an average side length of 18 nm. The perfection of such crystalline whiskers has been confirmed by TEM lattice imaging[6,7].

AFM has been shown to produce artifacts due to the convolution of the tip dimensions with the sample dimension[8]. The tip scan rate also influences the AFM image. These effects will be illustrated on samples of known geometry. The AFM imaging of cellulose at the surface of *V. ventricosa* microfibrils at molecular resolution under ambient conditions will also be reported.

Experimental

Sample preparation. Samples of *V. ventricosa* preserved in formaldehyde were washed successively in aqueous sodium hydroxide, distilled water, dilute hydrochloric acid and distilled water as described by Gardner and Blackwell[9]. The purified *V. ventricosa* cell wall was soaked in concentrated sulphuric acid (67% wt/wt) for 30 min at room temperature and a further 30 min at 70°C. It was subsequently washed in distilled water until neutral. Colloidal suspensions (~ 1 wt%) were then obtained by ultrasonic treatment for 2 min with a Branson model 350 sonifier.

A drop of the colloidal suspension of microfibrils in distilled water was placed on a carbon-coated TEM grid. After the water had evaporated, the grid was placed in an Edwards E306 vacuum coater and one half of the grid was coated with gold. The gold boundary was used to help locate specific microfibrils for AFM and TEM imaging. Samples were also prepared on a mica substrate. A drop of suspension of each of the samples in distilled water was placed on freshly cleaved mica, and the water was allowed to evaporate.

Atomic force microscopy. A Nanoscope II[3] AFM microscope was used to image *V. ventricosa* cellulose microfibrils on both carbon-coated copper grids and on mica substrates. The samples were scanned with a 100 μm long cantilever[3] at room temperature in both the height and force modes. In the height mode, the feedback gain to the z-axis (vertical) piezoelectric transducer is set at a high value so that the tip deflection is minimized ('constant' force), and the vertical motion of the piezoelectric transducer is recorded. In the force mode, the feedback gain to the z-axis transducer is set at a low value so that the z-axis piezo movement is minimized ('constant' height) and the cantilever deflection is recorded. All scans were recorded as 400×400 pixel images. An optical microscope was used to view the grid and hence to locate specific areas of the sample.

Transmission electron microscopy. A transmission electron microscope (Philips EM 400T) was used at an accelerating voltage of 120 kV. A first series of images

---

*To whom correspondence should be addressed

were obtained at low magnification ($\times 280$) and low electron dose conditions to minimize radiation damage. This series of images were taken along the gold boundary. The grid was then attached to a metal disc and transferred to the atomic force microscope. After images of some of these boundary areas were obtained with the atomic force microscope, the grid was reinserted into the transmission electron microscope for imaging the same areas by diffraction contrast. For this latter technique, a thin foil objective aperture ($20\ \mu m$ diameter) was used. In order to maintain the crystallinity of the specimen during observation, the microscope was operated at low dose intensity by overfocusing the first condenser lens.

Results and discussion

Figure 1a shows a TEM image of a group of microfibrils on a carbon film and *Figure 1b* shows the AFM image of the same area on the film. Obviously, the overall images are virtually identical. The AFM image clearly shows deposits of adventitious material on the grid surface that are not easily visible in the TEM image. However, the apparent width of the microfibrils in the AFM image seems too large. A TEM image of a section of the *V. ventricosa* cell wall is shown in *Figure 2*. The cross-sections of individual microfibrils are clearly visible; where the microfibrils are orthogonal to the microtome section, they appear as bright squares, with
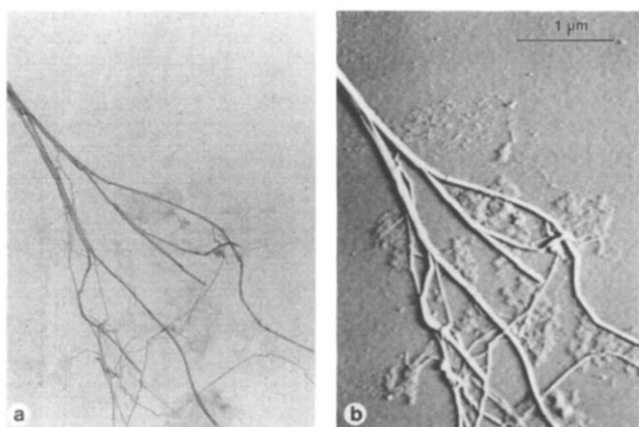

Figure 3 AFM micrograph cross-section of a single *V. ventricosa* cellulose microfibril
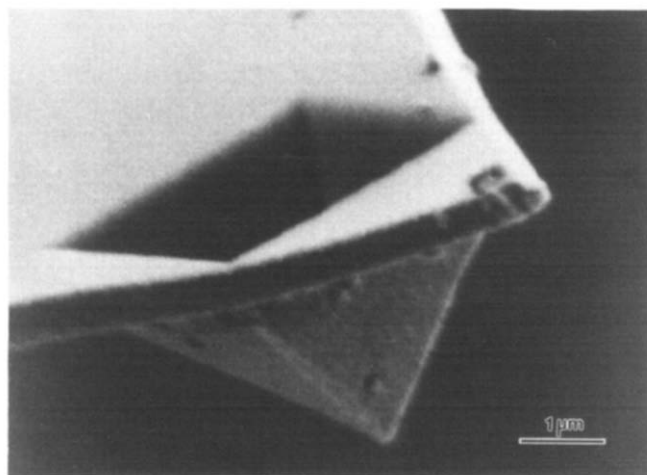
Figure 4 SEM micrograph of the AFM cantilever and tip, showing the rounded point of the pyramidal tip

Figure 1 (a) TEM micrograph and (b) AFM micrograph of *V. ventricosa* cellulose microfibrils on carbon-coated copper grids (tip velocity $10^5\ nm\ s^{-1}$)
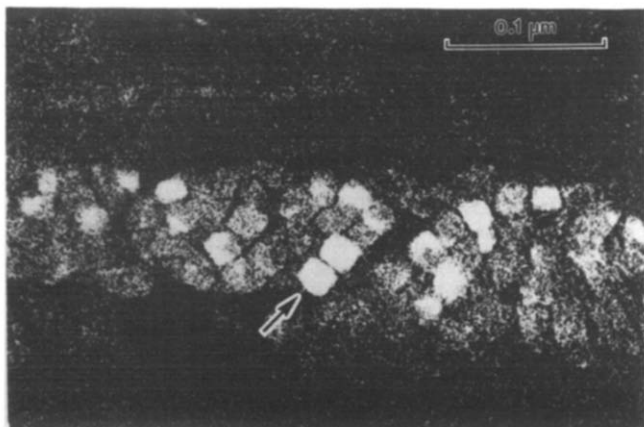

Figure 2 TEM cross-section of a portion of the cell wall of *V. ventricosa*. The square cross-section of an individual microfibril is indicated
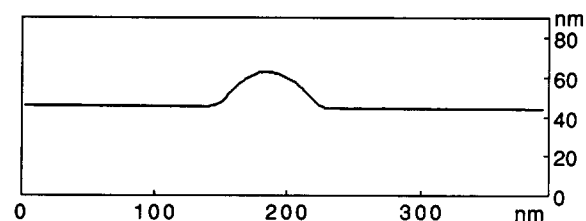
sides[5] of ~ 18 nm. The overall height of the microfibrils from AFM measured at tip velocities below $10^5\ nm\ s^{-1}$ compares favourably with this dimension. However, a marked discrepancy in the width and cross-sectional shape of the microfibrils is apparent. Rather than the expected approximately square cross-section[5], the AFM cross-section (*Figure 3*) shows a bell-shaped curve with a base width of ~ 100 nm. The distortion is primarily due to convolution of the AFM tip shape with that of the microfibril cross-section. Similar effects have recently been reported for AFM images of polyethylene single crystals[8]. A scanning electron microscopy (SEM) image of an AFM tip (*Figure 4*) shows the pyramidal[8] silicon nitride crystal on the cantilever. The shape of the microfibril cross-section observed here indicates from simple geometric considerations that the AFM tip has a rounded end with an approximate radius of 50 nm. It is not possible to confirm this from *Figure 4*. Care is obviously required in determining the dimensions of objects of this order of magnitude by AFM.

A second factor that must be considered is the AFM scan rate, or more precisely the tip velocity [tip velocity ($nm\ s^{-1}$) = scan rate (Hz) $\times$ length of scan (nm) $\times$ 2]. AFM images of *V. ventricosa* cellulose microfibrils on a mica substrate were recorded over the full range of scan rates with a large scan size of 5400×5400 nm. Three 700×700 nm areas of these recorded images, each containing one fibre, were then examined. Care was taken to ensure the same cross-section of each microfibril was used for all scan rates. *Figure 5* shows that the apparent height of the cross-section depends on the tip velocity. The most reliable measurement of vertical displacement is presumably in the plateau region at the lowest tip

velocities ($<4 \times 10^3$ nm s^{-1}). There appears to be some 'overshoot' as the tip speed is increased, before the response drops off at very high tip speeds. The apparent cross-sections become flatter as the scan rate is increased (*Figure 6*). Both sample deformation and instrument response time may be responsible for the distortions at high scan rates.
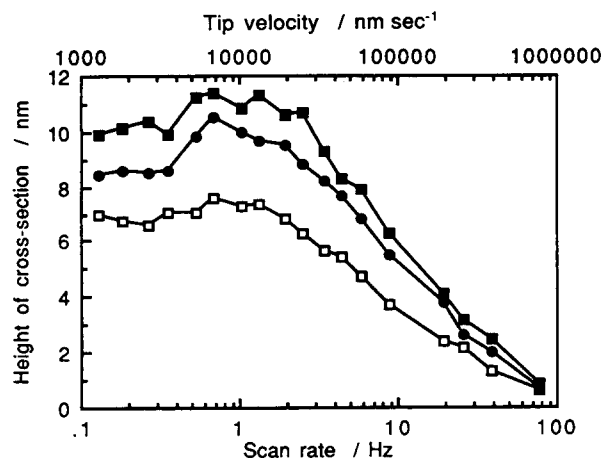
Figure 8 Representative AFM line profile of the surface of *V. ventricosa* cellulose microfibril

Figure 5 Plot of cross-sectional height of *V. ventricosa* cellulose microfibril against scan rate and tip velocity. Cross-sections of three different microfibrils are shown. Tip velocity (nm s^{-1}) = scan rate (Hz) × length of each scan (nm) × 2
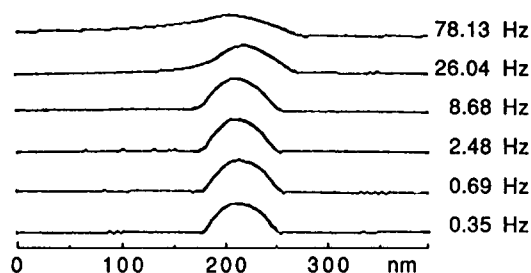
Figure 6 Series of cross-sections taken of the same microfibril at different scan rates, showing the change in height and base width with scan rate
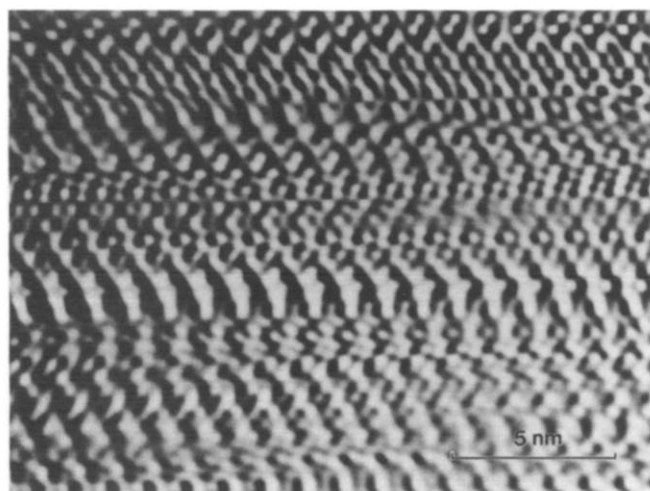
Figure 7 Two-dimensional fast Fourier transform AFM micrograph of the surface of *V. ventricosa* cellulose microfibril on mica. The fibre axis, and hence the cellulose chain direction, is horizontal. The microfibril was scanned along the fibre axis at a scan rate of 8 Hz, and no real-time filtering was applied
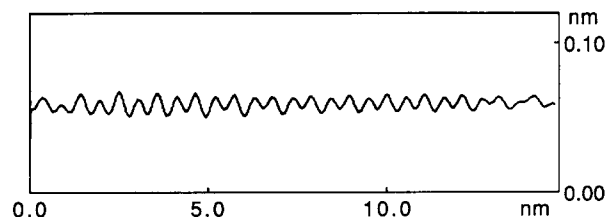
High resolution AFM imaging of the surface of a microfibril in height and force modes was performed at scan rates of 8 and 28 Hz, corresponding to tip velocities of 300 and 1000 nm s^{-1}, respectively. Care was taken to ensure that the area scanned was on the surface of the microfibril and not at the edge; as mentioned above, the base width of the apparent AFM cross-section is wider than that of the true cross-section due to the convolution of tip and sample shapes. One of the high resolution AFM images is shown in *Figure 7*. The microfibril was scanned parallel to its long axis, and hence to the cellulose chain direction. An apparent periodic structure is visible. Similar images were obtained on many microfibrils, as long as they were scanned parallel to the fibre direction. At other relative fibre/scan orientations, the images became featureless.

Line profiles along the microfibril axis, recorded over the entire image show reproducible periodicities of 1.07 and 0.53 nm (*Figure 8*). The unit cell of the 2_1 helix of *V. ventricosa* cellulose has a fibre repeat distance[10] of 1.038 nm, containing two glucose units. Thus the observed AFM periodicities of 1.07 and 0.53 nm may correspond to the fibre repeat and glucose unit repeat, respectively. The registry between neighbouring scans extends over a small distance, so that the lateral periodicity in *Figure 7* is very local. The absence of long-range lateral order almost certainly reflects the fact that at the outer surface of the crystallites, the cellulose chains are parallel to the fibre axis but show poor lateral registry.

Conclusions

AFM and TEM images of well characterized cellulose microfibrils show the complementary nature of these techniques. Despite the distortions in apparent dimensions caused by convolution of tip and sample geometries, AFM provides a unique and rapid indication of surface topography under ambient conditions, at length scales down to the atomic. Preliminary AFM measurements show periodicities along the microfibril axis that correspond to the fibre and glucose unit repeat distances.

References

1 Binnig, G., Quate, C. F. and Gerber, Ch. *Phys. Rev. Lett.* 1986, 12, 930
2 Gould, S. A. C., Drake, B., Prater, C. B., Weisenhorn, A. L., Manne, S., Hansma, H. G., Hansma, P. K., Massie, J., Longmire, M., Elings, V., Dixon, B., Northern, B., Mukergee, B., Peterson, C. M., Stoeckenius, W., Albrecht, T. R. and Quate, C. F. *J. Vac. Sci. Technol.* 1990, A8, 369

3   Nanoscope II Manual, Digital Instruments, Inc., Santa Barbara, 1990
4   Preston, R. D. 'The Physical Plant Biology of Plant Cell Walls', Chapman and Hall, London, 1974
5   Revol, J.-F. *Carbohydrate Polym.* 1982, **2**, 123
6   Sugiyama, J., Harada, H., Fujiyoshi, Y. and Uyeda, N. *Mokuzai Gakkaishi* 1984, **30**, 98
7   Revol, J.-F. *J. Mater. Sci. Lett.* 1985, **5**, 1347
8   Patil, R., Kim, S.-J., Reneker, D. H. and Weisenhorn, A. L *Polym. Commun.* 1990, **31**, 455
9   Gardner, K. H. and Blackwell, J. *J. Polym. Sci.* 1971, **C36**, 327
10   Gardner, K. H. and Blackwell, J. *Biopolymers* 1974, **13**, 1975